EFFECTIVENESS OF RF PHASE MODULATION FOR INCREASING BUNCH LENGTH IN ELECTRONS STORAGE RINGS

F. ORSINI, CEA SACLAY, Gif-sur-Yvette, France
A. MOSNIER, Projet SOLEIL, Gif-sur-Yvette, France

Abstract

Aiming at increasing the apparent bunchlength and hence the beam life time in electrons storage rings, RF phase modulation near one parametric resonance has been experimentally investigated. Since the possible benefit of this technique depends greatly on the ring parameters, we studied the effect of such a modulation for different RF parameters on the longitudinal emittance. Theoretical predictions and results of simulations are compared and discussed. It is shown that synchrotron radiation tends to spoil the parametric resonance. In particular, a criterion for islands survival has been found.

1 Introduction

In order to reach very high brilliance, Synchrotron Radiation Light Sources demand intense bunches with very small transverse and longitudinal emittances. However the high density of electrons increases the Touschek effect (e^-,e^- collisions at large angle) and thus reduces the beam lifetime. In order to reduce the electron density, different approaches have been considered: a higher harmonic cavity operating in the bunch lengthening mode or a RF phase modulation [1] which increases the apparent bunchlength but also the energy spread of the beam. This paper focuses on the second method, especially near the third-integer resonance, more appropriate than the integer resonance. The latter, widely explained in previous papers [2], is too strong to be useful in storage rings - distinct bunchlets with large spacing are formed - and is briefly discussed in Chapter 2. The

third-integer resonance, more promising, can be controlled through the two modulation parameters, frequency ω_m and amplitude A_m, which must be first properly chosen. Analytical expressions of fixed points and island widths are given in Chapter 3 and help for the optimization of the modulation. For illustration, three Synchrotron Light Sources are compared: BESSY I, SOLEIL and Super-ACO. Lastly, the combined effect of both synchrotron radiation and parametric resonance is studied in Chapter 4. Islands created by RF modulation tend to vanish as soon as radiation damping is introduced. A criterion, which guarantees island formation is then inferred from the Fokker-Planck equation. The validity of the criterion is finally tested with different parameters of the three machines.

2 Integer Resonance

The integer resonance has been thoroughly analysed in [2]. The particle motion can be characterized by three regimes according to the value of modulation tune, with respect to a bifurcation frequency, given by:

$$\omega_c = \omega_s[1 - \tfrac{3}{16}(4\,A_m)^{2/3}]$$

with ω_s the synchrotron frequency and A_m the amplitude of the perturbation of the first harmonic.

Well-below the bifurcation frequency ω_c, two stable fixed points define two well separated domains, that particles fill with about the same proportion. Above ω_c, only the farthest stable fixed point is left and the particles diffuse towards this off-centered island.

The three regimes of the integer resonance have been simulated with the parameters of the SOLEIL storage ring. Figure 1 shows for example the gathering of particles, initially uniformly distributed in phase space, into the islands after

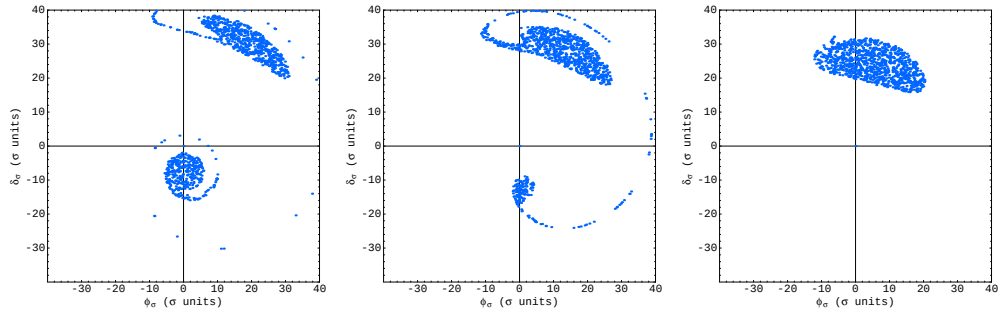

(a) well-below the bifurcation frequency

(b) just below the bifurcation frequency

(c) above the bifurcation frequency

Figure 1: Particles in normalized phase space (ϕ, δ) with RF phase modulation at the integer resonance.

a few damping times for different modulation tunes. As soon as the modulation amplitude is large enough so that the integer resonance takes place, dipole oscillations of large magnitude are created, whatever the regime. The integer parametric resonance is definitively not an appropriate method for decreasing the electron density of the bunch.

3 Third-integer resonance

3.1 Hamiltonian of the third-integer resonance: $\omega_m \approx 3\omega_s$

Only the main results are recalled hereafter and detailed derivations can be found in Appendix A. We consider a phase modulation with frequency close to three times the synchrotron frequency. The complete perturbated Hamiltonian, as a function of the phase ϕ and the energy deviation δ of one particle can be written as:

$$\begin{aligned} H(\phi,\delta) = {} & \tfrac{\omega_s}{2}\,\delta^2 + \omega_s \tan\overline{\phi_s}(\sin\phi\cos(A_m \sin\omega_m t) + \cos\phi\sin(A_m \sin\omega_m t)) \\ & -\omega_s\cos\phi\cos(Am\sin\omega_m t) + \omega_s\sin\phi\sin(A_m\sin\omega_m t) - \omega_s\phi\tan\overline{\phi_s} \end{aligned} \quad (1)$$

where ω_s is the synchrotron frequency and we define $\overline{\phi_s} = \pi - \phi_s$ with ϕ_s the synchronous angle.

We examine the Hamiltonian in the coordinate frame, rotating at the modulation frequency, by using the action-angle variables $(\tilde{J}, \tilde{\psi})$ defined as:

$$\delta = -\sqrt{2\,\tilde{J}}\,\cos(\tilde{\psi} + \omega_m\, t/3),\ \phi = -\sqrt{2\,\tilde{J}}\,\sin(\tilde{\psi} + \omega_m\, t/3)$$

Expanding into Bessel functions and assuming to be close to the third-integer parametric resonance, the time-averaged Hamiltonian, representing the motion invariant, takes the simple form:

$$< K >_t = (\omega_s - \frac{\omega_m}{3})\,\tilde{J} - \frac{\omega_s\,\tilde{J}^2}{16} - \frac{\omega_s\,A_m\,(2\tilde{J})^{3/2}}{48}\cos 3\tilde{\psi} - \omega_s \qquad (2)$$

In addition to the first linear term of the third-integer resonance, the hamiltonian comprises higher order functions of $\tilde{J}$. The cosine term provides the $\tilde{\psi}$-periodicity of $2\pi/3$. The terms, like ω_s, which do not depend on $\tilde{J}$ and $\tilde{\psi}$, do not affect the differential equations and can hence be ignored. In the new phase space $(\tilde{J}, \tilde{\psi})$, the stationary trajectories are given by the K-constant contours.

Position and width of the three islands, which determine the phase space occupied by the beam, are controlled by the modulation parameters and must be properly adjusted.

3.2 Fixed Points

The coordinates $(\phi_\sigma, \delta_\sigma)$ of the three stable fixed points are (for $\tilde{\psi} = 0,\ \frac{2\pi}{3},\ \frac{4\pi}{3}$):

$$\begin{array}{c} \delta_\sigma = \frac{a_m}{2}[1 + R_{FP}], \quad -\frac{a_m}{4}[1 + R_{FP}], \quad -\frac{a_m}{4}[1 + R_{FP}] \\ \phi_\sigma = 0, \quad \sqrt{3}\cdot\frac{a_m}{4}[1 + R_{FP}], \quad -\sqrt{3}\cdot\frac{a_m}{4}[1 + R_{FP}] \end{array} \qquad (3)$$

with the factor $R_{FP} = \sqrt{1 + \frac{64\,Q_s^2}{a_m^2(\sigma_\epsilon h\alpha)^2}\cdot(1 - \frac{\omega_m}{3\omega_s})}$, where a_m is the normalized modulation amplitude (A_m is in units of rms bunchlength), Q_s is the synchrotron tune, σ_ϵ is the natural energy spread, α is the momentum compaction and h is the harmonic number.

The fixed points position depends on ring and RF modulation parameters. In order to depopulate the bunch center as much as possible, islands have to be large enough on one hand, and to be placed close to the bunch core on the other hand. However, the previous equation (3) shows that the stable fixed points can never reach the origin, even for a vanishing distance to the resonance $(\omega_m - 3\,\omega_s)$ and are bounded by the lower limit a_m. Figure 2 illustrates this limit.

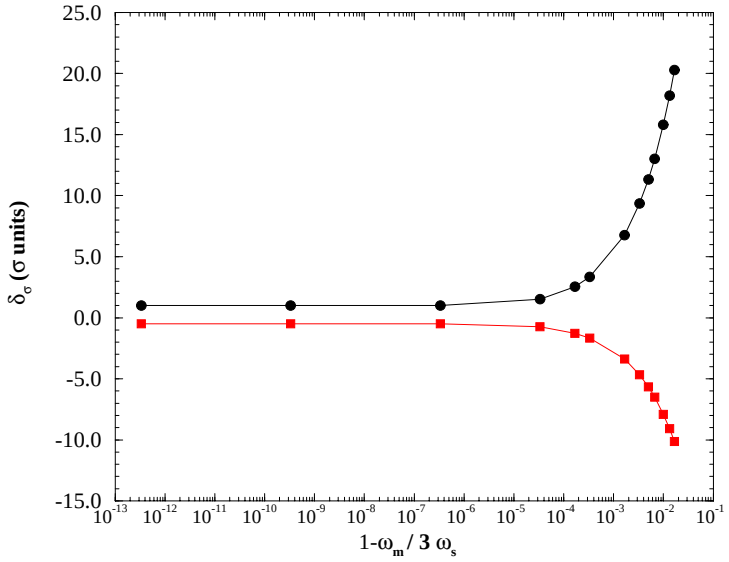

Figure 2: SOLEIL: Evolution of the amplitude δ_σ of the stable fixed point versus the third-integer resonance coefficient $(1 - \omega_m/3\,\omega_s)$.

3.3 Island width

The island width is given by the distance between the separatrice, curve joining the unstable fixed points, and the stable fixed points, where the hamiltonian is maximum [3]. The normalized width (in σ units) expressed in terms of storage ring parameters is given by:

$$\Delta\,\delta_\sigma = \pm\,16\sqrt{\frac{2}{3}}\cdot\left(\frac{Q_s}{\alpha\,\sigma_\epsilon\,h}\right)^{3/2}\cdot(1-\omega_m/3\,\omega_s)^{3/4}\times\frac{1}{\sqrt{a_m}\cdot R_{FP}} \qquad (4)$$

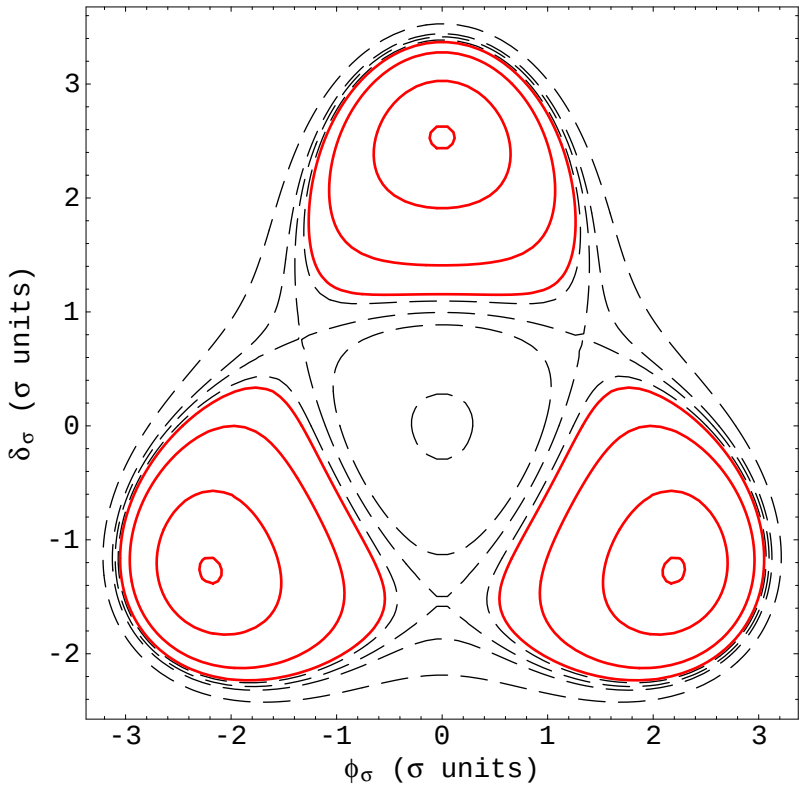

Figure 3: K-constant contours plotted in normalized phase space (ϕ, δ) for SOLEIL ring parameters (curves surrounding the stable fixed points are in solid lines and curves surrounding the unstable fixed points are in dashed lines).

The K-constant contours, calculated for the SOLEIL ring, are shown in figure 3. At small amplitude, the motion is nearly not affected by the resonance. Moving away from the origin, the circles become more and more distorted, until reaching the islands. The expression (4) reveals that the more ω_m tends to $3\,\omega_s$, the more the island width is reduced. The width is drawn in Figure 4 as a function of the distance to the resonance and scales as the power one quarter. There is then a trade-off between island position (ω_m very close to $3\,\omega_s$) and the island width (ω_m not too close to $3\,\omega_s$).

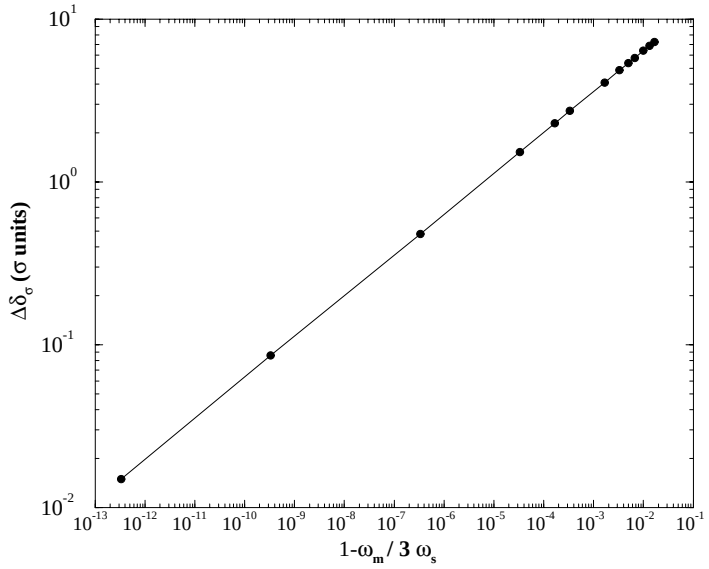

Figure 4: $\Delta\,\delta_\sigma$ in σ units versus the modulation frequency coefficient $(1 - \omega_m/3\,\omega_s)$.

3.4 Chirikov criterion

The Chirikov criterion [4] is used to estimate the onset of stochastic instability. In particular, chaotic behavior can occur when islands of two successive parametric resonances are too close and the overlap of resonances begins when their separatrices are in contact. As we will see later, this chaotic motion has been observed in some simulations with SOLEIL parameters.

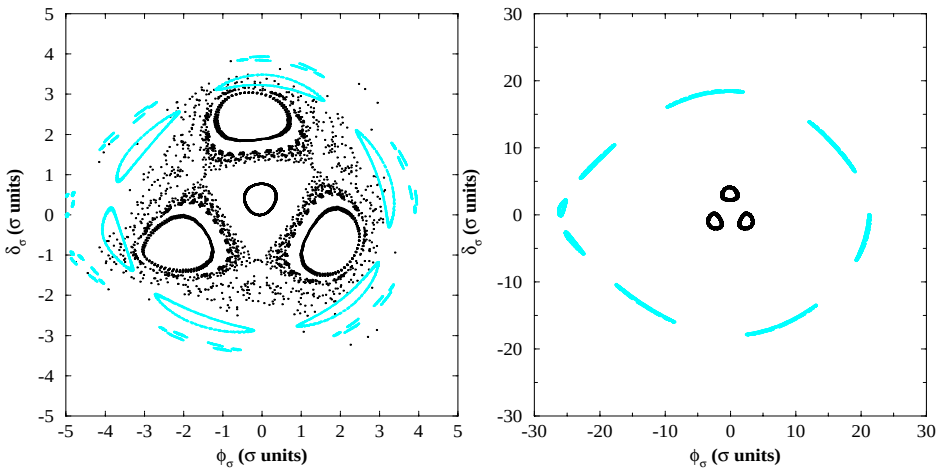

(a) chaotic behaviour (b) nonchaotic behaviour

Figure 5: Single bunch tracking in normalized phase space $(\phi_\sigma, \delta_\sigma)$. Dark points represent the third-integer resonance effect, grey points represent the fifth-integer resonance effect.

The Chirikov criterion is given by [4]:

$$\Delta\tilde{J}_1 + \Delta\tilde{J}_2 \; << \; \delta\tilde{J} \tag{5}$$

where $\Delta\tilde{J}_1$ and $\Delta\tilde{J}_2$ are the island widths of the third-integer and the fifth-integer resonances, respectively, and $\delta\tilde{J}$ is the island spacing in amplitude.

In case of RF phase modulation, and possible interaction between the third- and fifth-integer resonances, the criterion becomes:

$$(\tfrac{A_m}{6})^{1/2} \times (1 - \tfrac{\omega_m}{3\,\omega_s})^{3/4} \; << \; \tfrac{\Delta\omega_s}{\omega_s}$$

with $\Delta\omega_s/\omega_s = 1/6\,m^2$ and $m = 3$ for the third-integer resonance.

Expressed in terms of the normalized modulation amplitude, the condition on the modulation tune for a nonchaotic behaviour can be written as:

$$\frac{\omega_m}{\omega_s} \; >> \; 3 \times [1 - [\frac{1}{54}(\frac{6\,\omega_s}{\omega_{RF}\,\alpha\,\sigma_\epsilon\,a_m})^{1/2}]^{4/3}] \tag{6}$$

Figure 5 reproduces two numerical simulations for SOLEIL (chaotic behaviour) and for BESSY I (nonchaotic behaviour). In a nonchaotic behaviour, the fifth-

integer resonance has islands very far from the third-integer one, more than $15\,\sigma$ (figure 5-b) with small widths, in comparison to the island spacing. The particles are then independently governed by each resonance. Conversely, the fifth-integer islands hit the separatrices of the third-integer islands in case of chaotic behaviour (figure 5-a). The particles can then diffuse from one resonance to the next one, leading to particle loss.

3.5 Optimization of the RF phase modulation parameters

The modulation parameters, frequency ω_m and amplitude A_m, have been first optimized with the help of the analytical expressions (3) and (4), together with different storage ring parameters [5]. Table 1 summarizes the relevant parameters used for three light sources: SOLEIL, BESSY I and SuperACO.

	SOLEIL	**BESSY I**	**SuperACO**
Frequency (MHz)	352.2	499.2	100.0
Harmonic Number	396	104	24
Momentum Compaction	$4.77 \cdot 10^{-4}$	$1.5 \cdot 10^{-2}$	$1.48 \cdot 10^{-2}$
Nominal Energy (MeV)	2500	800	800
Energy loss/turn (keV)	800	20	21.3
Total RF Voltage (MV)	3.8	0.2	0.17
Longitudinal Damping Time (ms)	4.33	10.0	8.5
Natural Energy Spread	$9.24 \cdot 10^{-4}$	$5.0 \cdot 10^{-4}$	$5.5 \cdot 10^{-4}$
Bunchlength/wavelength: σ_L/λ_{RF} (%)	2	7.9	4.5

Table 1: Synchrotron Light Sources main parameters.

Both parameters, amplitude A_m and frequency ω_m of RF phase modulation, are given in table 2 after optimization. The corresponding stationary trajectories are plotted in figure 6. It is worth noting that the a_m value is moderate for preventing any coherent motion of the whole bunch and that the fixed points are close enough to the bunch core, while keeping a sufficient island width.

When the bunch is short compared to the RF wavelength, especially for SOLEIL, the modulation frequency has to be moved very close to $3\,\omega_s$ in or-

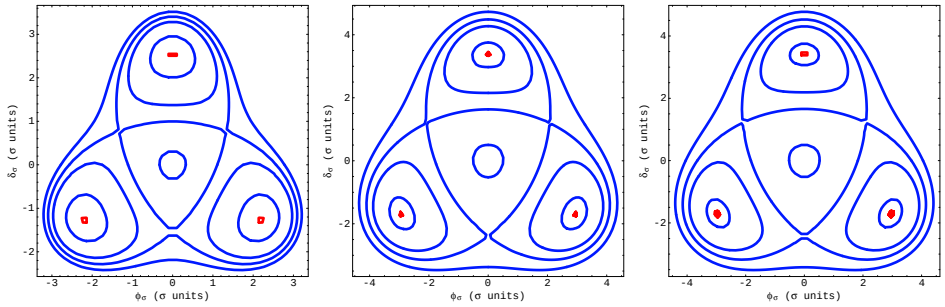

(a) Soleil (b) Bessy I (c) SuperAco

Figure 6: Separatrices and K-constant contours in normalized phase space $(\phi_\sigma, \delta_\sigma)$ with RF phase modulation of the third-integer.

	SOLEIL	**BESSY I**	**SuperACO**
ω_m/ω_s	2.9995	2.9850	2.9950
A_m (degrees)	1.48	5.68	3.24
SFPs coordinates $(\phi_\sigma, \delta_\sigma)$	$(0, +2.54)$ $(+2.20, -1.27)$ $(-2.20, -1.27)$	$(0, +3.39)$ $(+2.94, -1.69)$ $(-2.94, -1.69)$	$(0, +3.43)$ $(+2.97, -1.71)$ $(-2.97, -1.71)$
Island width (σ units)	2.29	2.71	2.77

Table 2: Final optimization of the RF phase modulation parameters and islands characteristics for each machines.

der to draw the fixed points to the origin. With these optimized parameters, we note that the particles, initially located at $1\,\sigma$, will be drawn out up to nearly $3\,\sigma$ for the three machines. A significant bunchlengthening is therefore expected.

4 Synchrotron radiation effect

In the previous analytical treatment, the synchrotron radiation effect, including radiation damping and quantum excitation, has not been taken into account. However, this effect cannot be neglected in storage rings, where these terms can be as large as the parametric resonance terms.

4.1 Fokker-Planck treatment

Due to the dissipative nature of the system, the previous Hamiltonian treatment can not be directly applied in presence of synchrotron radiation. The present analysis is based on the Vlasov equation with the Fokker-Planck collision term:

$$\frac{\partial F}{\partial t} + \{H, F\} = R \tag{7}$$

where $F(\phi, \delta, t)$ is the distribution function of particles in the bunch, $R = \frac{\partial}{\partial \delta}(\gamma_d F \delta + \kappa \frac{\partial F}{\partial \delta})$ is the collision term describing the synchrotron radiation effect and $\{\cdots\}$ denotes the Poisson bracket term. K is the perturbated Hamiltonian, $\gamma_d = 1/T_{rad}$ is the radiation damping rate and κ is the quantic diffusion factor, related to γ_d with $\sigma_\epsilon = \sqrt{\frac{\kappa}{\gamma_d}}$.

With the help of the four partial derivatives:

$$\frac{\partial \tilde{J}}{\partial \delta} = -\sqrt{2\,\tilde{J}}\,\cos\tilde{\psi}, \quad \frac{\partial \tilde{J}}{\partial \phi} = -\sqrt{2\,\tilde{J}}\,\sin\tilde{\psi}, \quad \frac{\partial \tilde{\psi}}{\partial \delta} = -\frac{\sin\tilde{\psi}}{\sqrt{2\,\tilde{J}}}, \quad \frac{\partial \tilde{\psi}}{\partial \phi} = -\frac{\cos\tilde{\psi}}{\sqrt{2\,\tilde{J}}}$$

the new Fokker-Planck equation, in terms of $(\tilde{J}, \tilde{\psi})$ variables, is:

$$\frac{\partial F}{\partial t} + \frac{\partial F}{\partial \tilde{\psi}} \frac{\partial K}{\partial \tilde{J}} - \frac{\partial F}{\partial \tilde{J}} \frac{\partial K}{\partial \tilde{\psi}} = 2 \frac{\partial}{\partial \tilde{J}} [\gamma_d \tilde{J} F + \kappa \tilde{J} \frac{\partial F}{\partial \tilde{J}}] \tag{8}$$

Replacing K in eq. (8) by its expression in $(\tilde{J}, \tilde{\psi})$ variables, and as this equation has now a stationnary solution $(\partial F / \partial t = 0)$, then the problem is reduced to:

$$\begin{array}{c} \frac{\partial F}{\partial \tilde{\psi}} \times [(\omega_s - \omega_m/3) - \frac{\omega_s \tilde{J}}{8} - \frac{\omega_s A_m \cos 3\tilde{\psi}}{16} (2\tilde{J})^{1/2}] \\ = 2\kappa \tilde{J} \frac{\partial^2 F}{\partial \tilde{J}^2} + \frac{\partial F}{\partial \tilde{J}} \times [\frac{\omega_s A_m (2\tilde{J})^{3/2}}{16} \sin 3\tilde{\psi} + 2\gamma_d \tilde{J} + 2\kappa] + 2\gamma_d F \end{array} \tag{9}$$

We are interested in the part which contains the $\frac{\partial}{\partial \tilde{J}}$ derivatives. The separation needs to fix the variable $\tilde{\psi} = \tilde{\psi}_1$ in the rotating frame, and using the usual separating variables method $(F(\tilde{J}, \tilde{\psi}) = g(\tilde{\psi}) \times h(\tilde{J}))$, the equation can be written as:

$$a(\tilde{J}) \frac{\partial^2 h}{\partial \tilde{J}^2} + b(\tilde{J}) \frac{\partial h}{\partial \tilde{J}} + c(\tilde{J}) h = 0 \tag{10}$$

where

$$\begin{cases} a(\tilde{J}) & = 2\kappa \tilde{J} \\ b(\tilde{J}) & = 2[\frac{\omega_s A_m (2\tilde{J})^{3/2}}{32} \sin 3\tilde{\psi}_1 + \gamma_d \tilde{J} + \kappa] \\ c(\tilde{J}) & = 2\gamma_d \end{cases}$$

If the amplitude of the third-integer modulation is equal to zero, we find the well-known Haissinski steady state solution, where h describes a gaussian bunch:

$$h(\tilde{J}) = \frac{\gamma_d}{\kappa} e^{-\frac{\gamma_d}{\kappa} \tilde{J}} \text{ or } h(\phi, \delta) = \frac{\gamma_d}{\kappa} e^{-\frac{\gamma_d}{\kappa} (\frac{\phi^2 + \delta^2}{2})}$$

Finally, the bunch shape, given by the distribution $h(\tilde{J})$, will get the form: $A(\tilde{J}) \times e^{-\frac{b(\tilde{J})}{a(\tilde{J})}}$ (where $A(\tilde{J})$ is an amplitude term coming from the resolution of eq. (10)).

The relevant term $b(\tilde{J})$, which contains the third-integer resonance perturbation with the synchrotron radiation effect, will determine the bunch gaussian shape or the modulated shape by islands formation. Thus the RF phase modulation is still efficient if the magnitude of the first coefficient is larger than the two last coefficients.

4.2 Island formation criterion

The three coefficients of the bracket term are:

$$C_1 = \frac{\omega_s\, A_m\, (2\,\tilde{J})^{3/2}}{32}\, \sin 3\tilde{\psi}_1 \quad , \quad C_2 = \gamma_d\, \tilde{J} \quad , \quad C_3 = \kappa$$

The C_3 term, generally much smaller than C_1 and C_2, can be neglected.

When the modulation parameters are optimized to catch the particles located in the bunch core $(1\,\sigma)$, it is particularly interesting to estimate if the particles are attracted in the islands or if they stay damped. With physical phase space variables (ϕ, δ), and the assumption that 1σ particles are treated, then the coefficients can be written as:

$$C_1 = \frac{\omega_s\, A_m}{16}\, (\frac{\alpha\, h\, \sigma_\epsilon}{Q_s})^3 \quad , \quad C_2 = \frac{1}{T_{rad}}\, (\frac{\alpha\, h\, \sigma_\epsilon}{Q_s})^2 \quad ,$$

Expressing the perturbation amplitude A_m in σ units of the bunch, i.e. $A_m = a_m\, \sigma_\phi$ and a_m is an integer, we find a limit value of the radiation damping time for the formation of islands:

$$T_{rad} \; > \; \frac{16\, Q_s}{\omega_{RF}\, \alpha^2\, h\, a_m} \times \frac{1}{\sigma_\epsilon^2} \tag{11}$$

Whenever the radiation damping time will be larger, third-integer resonance dominates and islands will be formed.

4.3 Simulations of formation or destruction of islands

The validity of the island survival criterion has been checked for various parameters of the three previous machines with the help of a multi-particle tracking code, which simulates the motion of particles with RF phase modulation, synchrotron radiation and quantum excitation. The simulation is based on the following recursive equations:

$$\bullet\ \phi_{n+1} = \phi_n + 2\pi\, Q_s \times \delta_n$$
$$\bullet\ \delta_{n+1} = (1 - \frac{2}{T_{rad}F_0}) \cdot \delta_n + \frac{2}{\sqrt{T_{rad}F_0}}\,\sigma_\epsilon R_I - \frac{2\pi\, Q_s}{\cos\overline{\phi_s}}\,(\sin(\overline{\phi_s} + (\phi_{n+1} + A_m \sin\omega_m t)) - \sin\overline{\phi_s}) \quad (12)$$

where R_I is a random number of normal distribution and F_o the revolution frequency.

For each calculation, the RF phase modulation parameters (ω_m, a_m) have been first optimized to get well-shaped islands. Furthermore, in order to shorten the simulation time for the criterion checking, it is preferable to use the energy spread parameter σ_ϵ instead of T_{rad}. Thus the criterion is now written as: $\sigma_\epsilon > \sqrt{\frac{1}{T_{rad}} \times \frac{16\, Q_s}{\omega_{RF}\,\alpha^2\, h\, a_m}}$.

For each machine, island formation and destruction were looked for, by using two values of energy spread: the natural one and a fictive one, giving the reverse situation.

Figures 7, 8 and 9 give the particle distribution in phase space, showing the island destruction for Soleil (figure 7-left), SuperAco (figure 9-left) and the island formation for Bessy I (figure 8-right) with their natural energy spread. Table 3 summarizes the energy spread values, which were tested, as well as the limit value (natural energy spread are in bold characters). The energy spread of Su-

	SOLEIL	**BESSY I**	**SuperACO**
$\sigma_{\epsilon\, lim}$	$11.13\,10^{-3}$	$4.14\,10^{-4}$	$14.02\,10^{-4}$
Island formation	$\sigma_\epsilon = 15.0\,10^{-3}$	$\boldsymbol{\sigma_\epsilon = 5.0\,10^{-4}}$	$\sigma_\epsilon = 18.33\,10^{-4}$
$\omega_{m\,chaos}/\omega_{m\,modul}$	1.05	0.93	0.96
No Island	$\boldsymbol{\sigma_\epsilon = 9.24\,10^{-4}}$	$\sigma_\epsilon = 2.3\,10^{-4}$	$\boldsymbol{\sigma_\epsilon = 5.5\,10^{-4}}$
$\omega_{m\,chaos}/\omega_{m\,modul}$	0.81	0.89	0.89

Table 3: σ_ϵ parameter of island formation or island absence due to the strong damping force.

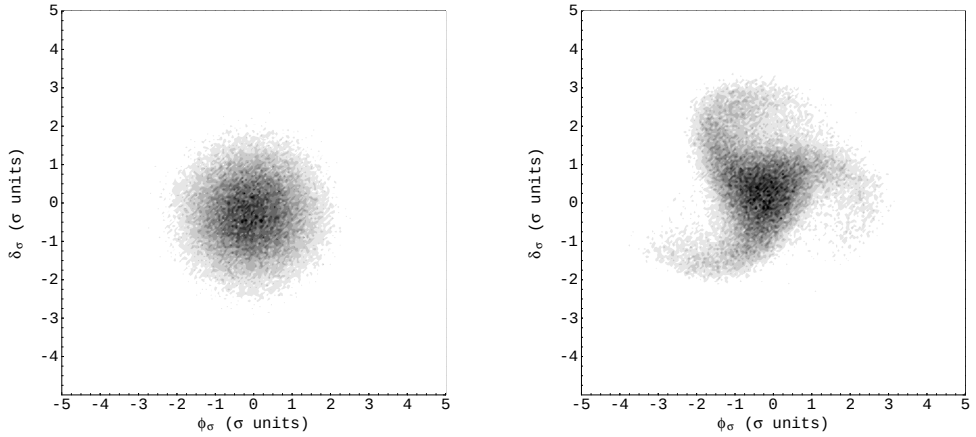

(a) Soleil: natural value of $\sigma_\epsilon = 9.24\,10^{-4}$.

(b) Soleil: $\sigma_\epsilon = 15.0\,10^{-3}$ modified for island formation in agreement with the criterion limit.

Figure 7: Snapshots (10^5 particles) in normalized phase space $(\phi_\sigma, \delta_\sigma)$ with island destruction (left) and island formation (right) for Soleil.

perAco, which was chosen for island creation, is larger than the natural one, but corresponds nevertheless to a real situation, when the beam current is well above the turbulent regime.

It is worthwhile noting that, the required energy spread for island formation is much higher for the SOLEIL ring than for the other ones, due mainly to the low value of the momentum compaction. In addition, assuming an energy spread larger than the limit value, chaotic motion and particle loss can be observed in Figure 7, as predicted by the Chirikov criterion (cf. Table 3).

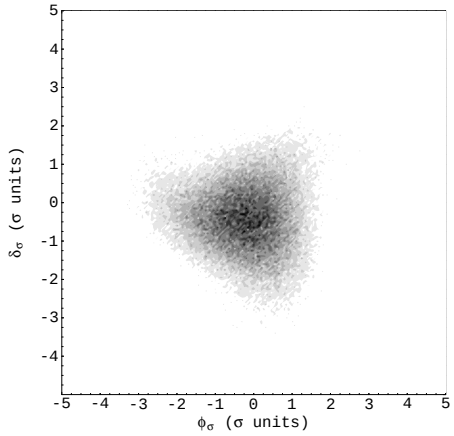

(a) Bessy I: $\sigma_\epsilon = 2.3\,10^{-4}$ modified for island destruction in agreement with the criterion limit.

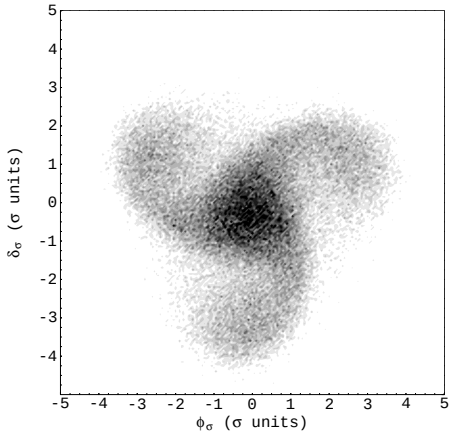

(b) Bessy I: natural value of $\sigma_\epsilon = 5.0\,10^{-4}$.

Figure 8: Snapshots (10^5 particles)in normalized phase space $(\phi_\sigma, \delta_\sigma)$ with island destruction (left) and island formation (right) for Bessy I.

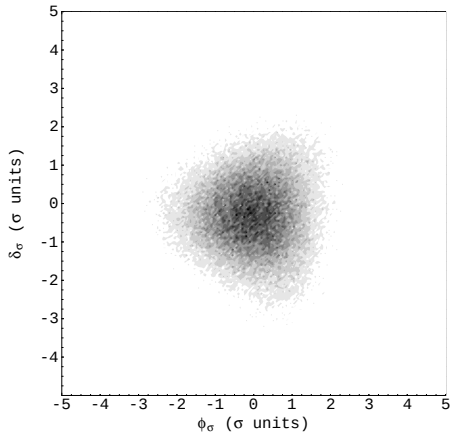

(a) SuperAco: natural value of $\sigma_\epsilon = 5.5\,10^{-4}$ for a bunch current equal to zero, there is island destruction in agreement with the criterion limit.

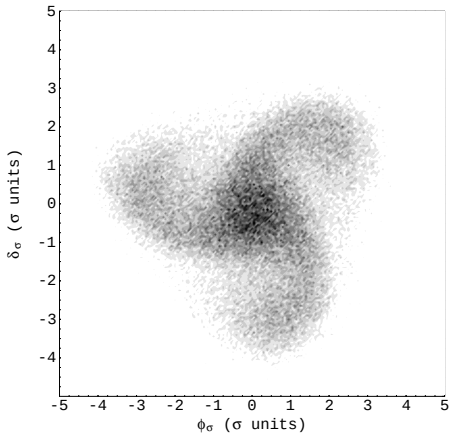

(b) SuperAco: natural value of $\sigma_\epsilon = 18.33\,10^{-4}$ for a bunch current equal to 60 mA, there is island formation in agreement with the criterion limit.

Figure 9: Snapshots (10^5 particles) in normalized phase space $(\phi_\sigma, \delta_\sigma)$ with island destruction (left) and island formation (right) for SuperAco.

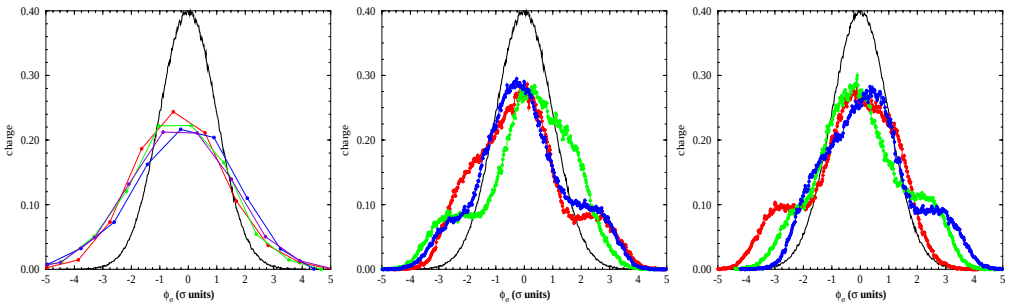

(a) Soleil: σ_ϵ modified (b) Bessy I (c) SuperAco

Figure 10: Distribution in charge versus the normalized angle ϕ_σ of a bunch of 100000 particles in situations where islands are formed.

Finally, figure 10 shows the enlarged charge distributions at different times , as well as the initial gaussian distribution for comparison. Except for SOLEIL, the net bunchlength has been increased by a factor between 2 and 3, but at the expense of a similar widening in energy spread, since islands are rotating in phase space at the modulation frequency ω_m.

5 Conclusion

With properly chosen parameters, the RF phase modulation method allows to enlarge the phase space occupied by the beam. However, the energy spread is also increased, by the same bunchlengthening factor. The Touschek lifetime can then be increased by a factor two, as it has been observed in BESSY I and ASTRID [6], but at the expense of beam quality, affecting in particular the brilliance in synchrotron light sources. In addition, synchrotron radiation effect can prevent island formation in some cases, which can be predicted by a criterion on the minimum required energy spread.

References

[1] V.V. Balandin, M.B. Dyachkov and E.N. Shaposhnikova, "The resonant theory of longitudinal emittance blow-up by phase-modulated high harmonic cavities", Part. Acc., vol. 35, pp.1-14 (1991).

[2] H. Huang and al.,"Experimental determination of the Hamiltonian for Synchrotron motion with rf phase modulation", Physical Review E, Vol. 48, N6, December 1993.

[3] R.D. Ruth,"Single-particle dynamics and nonlinear resonances in circular accelerators", Lecture Notes in Physics, Vol. 247, Springer Verlag, Proceedinds Sardinia 1985.

[4] B.V. Chirikov, "A universal Instability of Many-Dimensional Oscillators Systems", Phys. Report. 52, 1979.

[5] P. Kuske, Yu. Senichev, MP. Level: private communications.

[6] Yu. Senichev, N. Hertel, S. Lunt, S.P Moeller and J.S. Nielsen, "Increasing the life time of SR sources by rf phase modulation", Proceedings of the European Particle Accelerator Conference, Stockholm, Sueden (1998).

A APPENDIX

The properties of the Hamiltonian for the synchrotron motion with RF phase modulation are discussed. The longitudinal phase space will be transformed to action-angle coordinates, where the Hamiltonian in the rotating frame will be derived. We would explain why odd resonances are only considered and the complete perturbated Hamiltonian is calculated. Fixed points coordinates and island widths are derived in both frames (ϕ, δ) and $(\tilde{J}, \tilde{\psi})$.

The action angle of the perturbed hamiltonian (RF phase modulation with amplitude A_m and frequency ω_m)

$$\begin{cases} \frac{d\phi}{dt} & = \omega_s \times \delta \\ \frac{d\delta}{dt} & = -\frac{\omega_s}{\cos\overline{\phi_s}} \left(\sin(\overline{\phi_s} + (\phi + A_m \sin\omega_m t)) - \sin\overline{\phi_s}\right) \end{cases}$$

The complete perturbated Hamiltonian in (ϕ, δ) variables is given by:

$$\begin{array}{c} H_1(\phi,\delta) = \frac{\omega_s}{2}\,\delta^2 + \omega_s \tan\overline{\phi_s}(\sin\phi\cos(A_m\sin\omega_m t) + \cos\phi\sin(A_m\sin\omega_m t)) \\ -\omega_s\cos\phi\cos(Am\sin\omega_m t) + \omega_s\sin\phi\sin(A_m\sin\omega_m t) - \omega_s\phi\tan\overline{\phi_s} \end{array} \tag{13}$$

The first canonical tranformation in action-angle coordinates (J, ψ) gives the new Hamiltonian:

$$\begin{array}{c} H_1(J,\psi) = \omega_s\,J\sin\psi^2 + \omega_s\tan\overline{\phi_s}[\sin(\sqrt{2J}\cos\psi + A_m\sin(\omega_m t))] \\ -\omega_s[\cos(\sqrt{2J}\cos\psi + A_m\sin\omega_m t)] - \omega_s\tan\overline{\phi_s}(\sqrt{2J}\cos\psi) \end{array} \tag{14}$$

The perturbated Hamiltonian is much more complicated and the perturbated part is not clearly defined. The Hamiltonian, expanding into Bessel functions, is written as:

$$H_1(J,\psi) = \omega_s\,J\sin\psi^2 - \omega_s\,J_o(\sqrt{2J}) - 2\omega_s\textstyle\sum_{k=1}^{\infty}(-1)^k\cdot J_{2k}(\sqrt{2J})\cdot\cos(2k\psi)$$

$$-\omega_s\tan\overline{\phi_s}\sqrt{2J}\cdot\cos\psi + \omega_s\tan\overline{\phi_s}\,A_m\sin(\omega_m t)\cdot J_o(\sqrt{2J})$$

$$+2\omega_s \tan\overline{\phi_s} \sum_{k=0}^{\infty}(-1)^k \cdot J_{2k+1}(\sqrt{2J}) \cdot \cos((2k+1)\psi)$$

$$+\omega_s A_m \sum_{k=0}^{\infty}(-1)^k \cdot J_{2k+1}(\sqrt{2J}) \cdot \underbrace{[\sin(\omega_m t \pm (2k+1)\psi)]}_{\text{odd resonances}}$$

$$+\omega_s \tan\overline{\phi_s}\, A_m \sum_{k=1}^{\infty}(-1)^k \cdot J_{2k}(\sqrt{2J}) \cdot \underbrace{[\sin(\omega_m t \pm 2k\psi)]}_{\text{even resonances}}$$

All resonances appear: odd resonances $\sin(\omega_m t - (2k+1)\psi)$ and even resonances $\sin(\omega_m t - 2k\psi)$ (terms with plus sign are non-resonnant terms). All the terms containing $\tan\overline{\phi_s}$ are neglected in the following, because generally in storage rings, bunches are placed for the maximum RF acceptance, so the synchronous phase $\overline{\phi_s} \longrightarrow 0$. For this reason even resonances can be neglected, compared to the odd ones.

Study of the third-integer resonance: $\omega_m \approx 3\omega_s$

Assuming to be close to the third-integer resonance (k=1) and that all non-resonant terms in the Hamiltonian can be neglected, then the Hamiltonian becomes:

$$H_1(J,\psi) = \omega_s J - \tfrac{\omega_s J^2}{16} - \omega_s - \tfrac{\omega_s J}{2}\cos 2\psi - 2\omega_s \sum_{k=1}^{\infty}(-1)^k \cdot J_{2k}(\sqrt{2J}) \cdot \cos(2k\psi)$$
$$-\omega_s A_m \cdot J_3(\sqrt{2J}) \cdot \sin(\omega_m t - 3\psi)$$

H_1 is time dependant again. A new canonical transformation in a rotating system in phase space suppress this constraint. The generating function of the second type is used for the new transformation:

$$F_2(\tilde{J},\tilde{\psi}) = (\psi - \tfrac{\omega_m t}{3} - \tfrac{\pi}{2}) \times \tilde{J}$$

with $\tilde{J} = J$ and $\tilde{\psi} = \psi - \omega_m\, t/3 - \pi/2$.

The new hamiltonian K is independant of the time, thus it is a constant of the motion:

$$K = H_1 + \frac{\partial F_2}{\partial t} = H_1 + (-\frac{\omega_m}{3})\,\tilde{J}$$

In the rotating frame, the particle trajectories are described by the total time-averaged Hamiltonian K:

$$< K >_t = (\omega_s - \frac{\omega_m}{3})\,\tilde{J} - \frac{\omega_s\,\tilde{J}^2}{16} - \frac{\omega_s\,A_m\,(2\tilde{J})^{3/2}}{48}\cos 3\tilde{\psi} - \omega_s \qquad (15)$$

Terms in the Hamiltonian which are not functions of $\tilde{J}$ and $\tilde{\psi}$ do not affect the differential equations for $\tilde{J}$ and $\tilde{\psi}$ and thus can be ignored in the following (ω_s is also forgotten).

Fixed Points Calculation

These fixed points are obtained by the following conditions:

$$\begin{cases} \frac{d\tilde{J}}{dt} &= -\frac{\partial K}{\partial \tilde{\psi}} = 0 \\ \\ \frac{d\tilde{\psi}}{dt} &= \frac{\partial K}{\partial \tilde{J}} = 0 \end{cases} \qquad (16)$$

With both equations, 6 fixed points are found for which the sign of $\cos 3\tilde{\psi}$ determines their stability or the instability:

- 3 Stable Fixed Points (SFPs) for $\tilde{\psi} = 0, \frac{2\pi}{3}, \frac{4\pi}{3}$.

  They are stable because the term $\cos 3\tilde{\psi}$ is positive, the potential has a minimum.

- 3 Unstable Fixed Points (UFPs) for $\tilde{\psi} = \frac{\pi}{3}, \pi, \frac{5\pi}{3}$.

  They are unstable because the term $\cos 3\tilde{\psi}$ is negative, the potential has a maximum.

The trajectories surrounding the stable fixed points are closed and formed islands of stability for particles, whereas the trajectories surrounding the UFP's are hyperbolics and these curves are separatrices, which are the boundaries of

the stable islands. In the new phase space $(\tilde{J}, \tilde{\psi})$, the stationary trajectories correspond to the K-constant contours.

The coordinates $(\phi_\sigma, \delta_\sigma)$ of the three stable fixed points are (for $\tilde{\psi} = 0,\ \frac{2\pi}{3},\ \frac{4\pi}{3}$):

$$\begin{array}{c} \delta_\sigma = \frac{a_m}{2}[1+R_{FP}], \quad -\frac{a_m}{4}[1+R_{FP}], \quad -\frac{a_m}{4}[1+R_{FP}] \\ \phi_\sigma = 0, \quad \sqrt{3}\cdot\frac{a_m}{4}[1+R_{FP}], \quad -\sqrt{3}\cdot\frac{a_m}{4}[1+R_{FP}] \end{array} \tag{17}$$

The coordinates $(\phi_\sigma, \delta_\sigma)$ of the three unstable fixed points are:

$$\begin{array}{c} \delta_\sigma = -\frac{a_m}{2}[1-R_{FP}], \quad -\frac{a_m}{4}[1-R_{FP}], \quad -\frac{a_m}{4}[1-R_{FP}] \\ \phi_\sigma = 0, \quad \sqrt{3}\cdot\frac{a_m}{4}[1-R_{FP}], \quad -\sqrt{3}\cdot\frac{a_m}{4}[1-R_{FP}] \end{array} \tag{18}$$

with the factor $R_{FP} = \sqrt{1 + \frac{64 Q_s^2}{a_m^2 (\sigma_\epsilon h \alpha)^2} \cdot (1 - \frac{\omega_m}{3\omega_s})}$, where a_m is the normalized modulation amplitude (A_m is in units of rms bunchlength), Q_s is the synchrotron tune, σ_ϵ is the natural energy spread, α is the momentum compaction and h is the harmonic number. When ω_m tends to $3\,\omega_s$, the UFPs coordinates are cancelled.

Islands width Calculation

The boundaries of the stable islands are formed by curves joining the unstable fixed points. As K is a constant of the curve, we can write: $K(\tilde{J}, \tilde{\psi}) = K(\tilde{J}_{UFP}, \tilde{\psi}_{UFP})$ where $\tilde{J}_{UFP}$ is the action at the unstable fixed points ; also on the separatrice we find:

$$(\tilde{J} - \tilde{J}_{UFP})^2 \simeq \frac{A_m \left(16\left(1 - \omega_m/3\,\omega_s\right)\right)^{3/2} \left(1 + \cos 3\tilde{\psi}\right)}{3} \tag{19}$$

The island width $\Delta\tilde{J}$ is given by the distance between the separatrice and the stable fixed poins, where the hamiltonian is maximum [3]:

$$\Delta\tilde{J} = \pm\, 8 \sqrt{\frac{A_m \cdot 2\left(1 - \omega_m/3\,\omega_s\right)^{3/2}}{3}}$$

For the easiest stable fixed point, where $\tilde{\psi} = 0$, and with the variable changing, $\Delta\tilde{J} = (\tilde{J}_{SFP} - \tilde{J}_{UFP}) = \frac{(\delta_{SFP}^2 - \delta_{UFP}^2)}{2}$ and $\delta_{SFP}^2 - \delta_{UFP}^2 = (\delta_{SFP} - \delta_{UFP})\,(\delta_{SFP} +$

$\delta_{UFP}) = \Delta\delta \times (\delta_{SFP} + \delta_{UFP})$, then the island width in phase space coordinates is:

$$\Delta\,\delta = \pm 16\,\sqrt{\frac{A_m \cdot 2(1-\omega_m/3\,\omega_s)^{3/2}}{3}} \times \frac{1}{\delta_{SFP}+\delta_{UFP}}$$

The island width, normalized in σ units and expressed with storage ring parameters, is:

$$\Delta\,\delta_\sigma = \pm 16\sqrt{\frac{2}{3}} \cdot (\frac{Q_s}{\alpha\,\sigma_\epsilon\,h})^{3/2} \cdot (1-\omega_m/3\,\omega_s)^{3/4} \times \frac{1}{\sqrt{a_m}\,R_{FP}} \qquad (20)$$

Generally, $\frac{64\,Q_s^2}{a_m^2(\sigma_\epsilon h\alpha)^2} \cdot (1-\frac{\omega_m}{3\omega_s}) >> 1$, then we can make approximation for eq. (20), so we obtain:

$$\Delta\,\delta_\sigma \simeq \pm 2\sqrt{\frac{2}{3}} \cdot (\frac{Q_s}{\alpha\,\sigma_\epsilon\,h})^{1/2} \cdot (1-\omega_m/3\,\omega_s)^{1/4} \times \sqrt{a_m} \qquad (21)$$

The island width grows with a_m, but it is reduced when ω_m tends to $3\,\omega_s$ ($\Delta\,\delta_\sigma \propto (1-\frac{\omega_m}{3\,\omega_s})^{1/4}$).